

Optimum Er concentration for *in situ* doped GaN visible and infrared luminescence

D. S. Lee, J. Heikenfeld, and A. J. Steckl^{a)}

Nanoelectronics Laboratory, University of Cincinnati, Cincinnati, Ohio 45221-0030

U. Hommerich, J. T. Seo, and A. Braud

Research Center for Optical Physics, Department of Physics, Hampton University, Virginia 23668

J. Zavada

U.S. Army European Research Office, London, United Kingdom

(Received 9 April 2001; accepted for publication 5 June 2001)

GaN thin films have been doped with varying Er concentrations (0.01–10 at.%) during molecular-beam-epitaxy growth. As expected, the visible and infrared (IR) emissions, from photoluminescence (PL) and electroluminescence (EL), are a strong function of Er concentration. We report on the determination of an optimum Er doping level for PL and EL intensity. Secondary ion mass spectroscopy and Rutherford backscattering measurements showed that the Er concentration in GaN increased exponentially with Er cell temperature. PL and EL intensity of green emission at 537 and 558 nm, due to Er $4f-4f$ inner shell transitions, exhibited a maximum at ~ 1 at. % Er. IR PL intensity at $1.54 \mu\text{m}$, due to another Er transition, revealed the same maximum for ~ 1 at. % Er concentration. PL lifetime measurements at 537 nm showed that samples with Er concentration < 1 at. % had a lifetime of $\sim 5 \mu\text{s}$. For Er concentration ≥ 1 at. %, the lifetime decreased rapidly to values below $1 \mu\text{s}$. This concentration quenching is believed to be due to a combination of Er cross relaxation and energy transfer to GaN defects, eventually followed by precipitation. This conclusion is supported by x-ray diffraction measurements. As a result, we have determined that the optimum Er doping concentration into GaN is ~ 1 at. %. © 2001 American Institute of Physics. [DOI: 10.1063/1.1390480]

Er-doped GaN is currently being widely studied¹ for its various optical applications. Due to the characteristic $1.54 \mu\text{m}$ infrared (IR) emission from Er^{3+} ions and minimum light absorption at this wavelength in silica, Er-doped silica-based optical fibers are now widely used. Many other materials, such as Si and various II–VI and III–V semiconductors, have been studied in order to find good Er host materials for optoelectronic applications. Favennec *et al.* reported² that Er^{3+} photoluminescence (PL) intensity depends strongly on both the band-gap energy of the semiconductor and the host temperature. The advantages of GaN include a direct-band-gap transition, which is very important in optical applications; a large energy band gap, which results in very low thermal quenching,^{3,4} and thermal and chemical robustness.

In addition to IR emission, Er also has characteristic emission in the visible range. We have previously reported⁵ visible green emission from Er-doped GaN thin films grown by molecular-beam epitaxy (MBE). We have observed that the visible and IR emission, from PL and electroluminescence (EL), are a strong function of Er concentration. In general, all Er host materials exhibit a practical limit in Er concentration beyond which the optical emissions begin to decrease. This is known as the concentration quenching effect. The limit, or optimum concentration of rare-earth ions, including Er, varies depending on the host materials. For example, the solubility limit of Er in Si is well known as

$\sim 10^{18} \text{cm}^{-3}$, while the PL intensity at $1.54 \mu\text{m}$ was reported⁶ to saturate at even a lower concentration of $\sim 5 \times 10^{18} \text{cm}^{-3}$, which is an Er concentration of $\sim 10^{-3}$ at. %. Other reported maximum Er concentrations include $\sim 5 \times 10^{18} \text{cm}^{-3}$ in GaAs (Ref. 7) and $4 \times 10^{19} \text{cm}^{-3}$ in Al_2O_3 .⁸ Although many experiments have been reported for GaN doped with Er, and a decrease of optical emission intensity at higher concentrations has been thought to be basically the same as in other hosts, no quantitative studies of the optimum Er concentration have been published. In this letter, we report on the optimum Er concentration in GaN for optical emission.

Er-doped GaN has been grown in a Riber 32 MBE system on *p*-type (111) Si substrates. A typical MBE growth cycle starts with the Si substrate preheated at 500°C in the preparation chamber and outgassed at 850°C for 10 min in the growth chamber. Electron diffraction showed clear 7×7 reconstruction patterns on the Si(111) surface after outgassing. A thin film of AlN was first grown for 5 min as a buffer followed by GaN:Er growth for 1 h at 700°C . Ga and Al elemental sources and a SVT Associates nitrogen rf-plasma source were used for growth. Er was introduced *in situ* during growth from a solid source. The Er concentration in the GaN film was varied by adjusting the Er cell temperature from 740 to 980°C . For electroluminescence measurements a simple ring-shaped Schottky electrode was fabricated on top of the GaN:Er film using indium–tin–oxide (ITO) sputtering and a lift-off process. The electrode has an

^{a)}Electronic mail: a.steckl@uc.edu

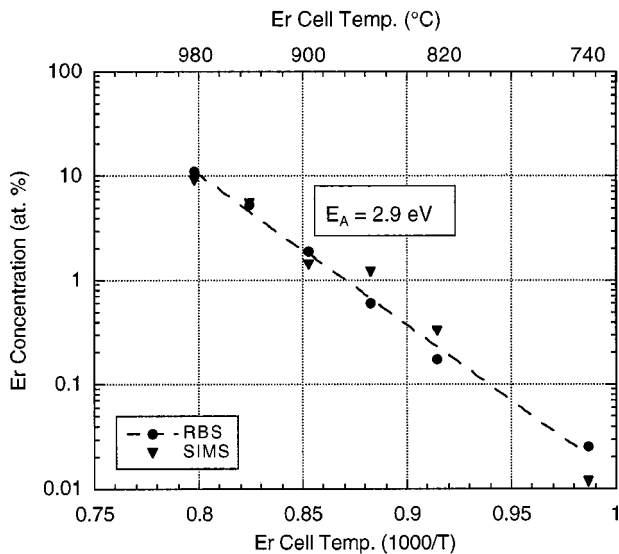


FIG. 1. Absolute Er concentration in GaN as measured by RBS and SIMS as a function of Er cell temperature. Measured activation energy of 2.9 eV coincides well with the value of ~ 3.0 eV for the vapor pressure of Er in this temperature range.

area of $7.65 \times 10^{-4} \text{ cm}^2$ and its detailed structure is shown elsewhere.⁹

Rutherford back scattering (RBS) and secondary ion mass spectroscopy (SIMS) measurements were used to measure absolute Er concentrations in GaN:Er films. Measurement results showed that the Er concentration in GaN ranged from 0.025 to 11.2 at. % by varying the cell temperature from 740 to 980 °C. As shown in Fig. 1, the incorporated Er concentration was observed up to the highest values measured. The Er concentration follows an exponential dependence on the Er cell temperature. An Arrhenius-like thermal activation energy estimated from this curve was 2.9 eV, which gives an excellent agreement with the activation energy of ~ 3.0 eV for the Er vapor pressure in this temperature.¹⁰

PL was performed at room temperature both in the visible and infrared regions by above-band-gap excitation with a 325 nm HeCd laser. Visible and IR PL intensities are plotted in Fig. 2(a). Green emission at 537 nm is one of the characteristic emissions due to the $4f-4f$ inner shell transition of Er^{3+} ions and is attributed to a transition from $^2H_{11/2}$ to $^4I_{15/2}$. IR emission at $1.54 \mu\text{m}$ is a well-known transition from $^4I_{13/2}$ to $^4I_{15/2}$ and has special importance because of current and potential optical communication applications. As shown in Fig. 2(a), both of these emissions have a maximum at about 1 at. % Er. It is well known in phosphor materials¹¹ that the optical excitation intensity of rare-earth activator ions exhibits an optimum concentration. The excitation residing in an ion can migrate to another ion of the same species that is in the ground state as a result of resonant energy transfer when they are located sufficiently close to each other. This process is known as cross relaxation. The energy migration process increases the possibility that the optical excitation is trapped at defects or impurity sites, enhancing nonradiative relaxation.

EL was investigated utilizing a Schottky device consisting of ITO ring electrodes on top of the GaN:Er layer. Brightness normalized by current flow, defined as BIV, is

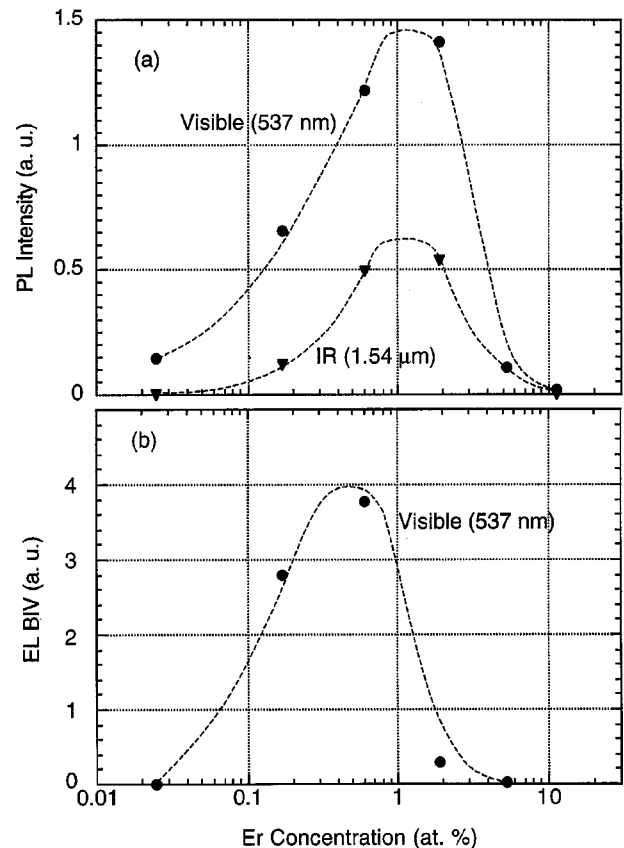


FIG. 2. PL and EL intensity vs Er concentration: (a) visible and IR PL intensity display maxima at ~ 1 at. % Er; (b) visible EL intensity normalized by current flow shows a maximum at ~ 0.5 at. % Er.

plotted in Fig. 2(b) for devices with various Er concentrations. Since the EL brightness was influenced by many factors, including those associated with EL device fabrication, the current normalized brightness is a more appropriate parameter to evaluate rather than the raw brightness, i.e., brightness regardless of current flow through the device at a fixed applied voltage. We can see that the optimum Er concentration is 0.5–1 at. % for visible EL emission, which is almost the same as that observed in PL.

The room-temperature PL lifetime was excited at 537 nm and measured at 558 nm. Below-band-gap excitation was used since above-band-gap excitation generated a yellow band emission around 550 nm and made it difficult to measure the lifetime of Er^{3+} . As shown in Fig. 3, the lifetime is constant at a value of $5 \mu\text{s}$ for low Er concentrations. At ~ 1 at. % Er, the lifetime starts to decrease with increasing concentration. The decrease of lifetime is most probably due to a cross relaxation of Er^{3+} ions in GaN. As observed in PL and EL intensity data, ~ 1 at. % Er concentration is a transition point at which cross relaxation and/or energy transfer become comparable to radiative emission.

Finally, x-ray diffraction (XRD) was carried out to investigate the crystal structure of the GaN:Er films. Figure 4 shows XRD spectra for four different samples, including undoped GaN as a reference. The (0002) characteristic peak of GaN at $2\theta = 34.5^\circ$ was observed to broaden in width and decrease in intensity as the Er concentration increased beyond $\sim 1-2$ at. %. Most interestingly, a new material phase appeared at 2θ of $\sim 32.1^\circ$ for the sample with 11.2 at. % Er.

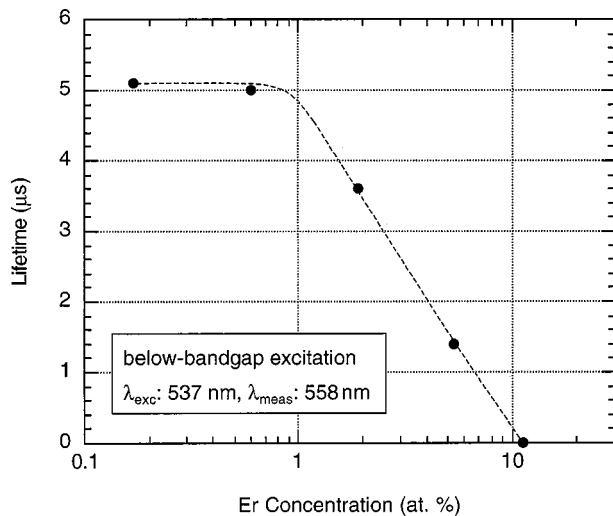


FIG. 3. Visible PL lifetime measurement at 537 nm with below-band-gap excitation as a function of Er concentration. Lifetime decreases rapidly for Er concentration greater than ~ 1 at. %.

The intensity of this XRD peak is an order of magnitude smaller than that of the main GaN peak. The peak was assigned to an ErN(111) diffraction and was broad. The intensity and full width at half maximum (FWHM) of the GaN(0002) peaks were plotted for all Er-doped samples in Fig. 5. We can clearly see that both the intensity and FWHM are constant at low Er concentrations until ~ 1 –2 at. % is reached. At higher Er concentrations, the XRD signal intensity decreased and the FWHM broadened. This implies that the GaN crystalline quality degradation begins at 1–2 at. % Er incorporation. Clearly, incorporation of Er at the ~ 10 at. % level significantly reduces the GaN crystallinity by precipitation of a new phase, ErN.

In summary, we have determined that there is an opti-

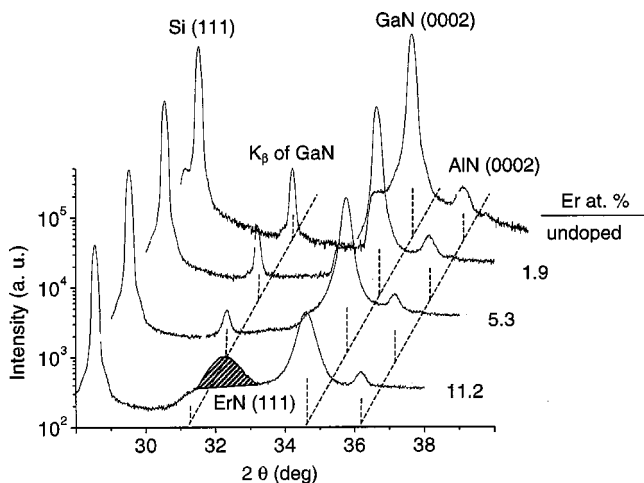


FIG. 4. X-ray diffraction (XRD) spectra from three samples doped with different Er concentrations and an undoped GaN sample as a reference. The main (0002) GaN peak is reduced in intensity and becomes broader as the Er concentration increases. For 11.2 at. % Er incorporation, a peak from a new material phase of ErN(111) appears.

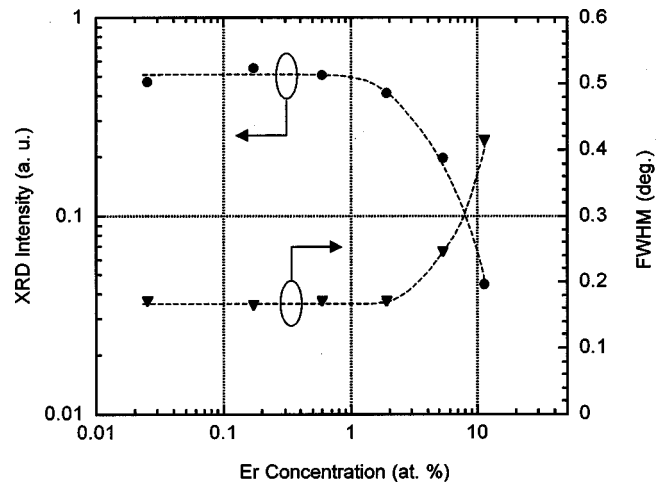


FIG. 5. XRD intensity and FWHM as a function of Er concentrations. The intensity becomes smaller and the FWHM increased beyond 1–2 at. % Er incorporation.

imum Er concentration in GaN:Er with regard to optical luminescence such as PL and EL. We conclude that the optimum Er concentration is ~ 1 at. % based on visible and IR PL, visible EL, visible PL lifetime, and XRD. It seems that two important things start to happen at around 1 at. % Er in GaN. The first is a combination of Er cross relaxation and energy transfer to GaN defects, resulting in the quenching of the luminescence. The second is the reduction in crystal structure quality which eventually produces a different phase, ErN, by precipitation. The ~ 1 at. % Er optimum concentration for maximum brightness is 2–3 orders of magnitude higher than that of Er in Si (Ref. 6) and GaAs,⁷ and about an order of magnitude higher than that of Er in Al₂O₃.⁸

At Cincinnati, this work was supported by ARO Grant No. DAAD 19-99-1-0348 and an ARO AASERT grant. Equipment support was provided by an ARO URI grant and the Ohio Materials Network. The work of Hampton University was supported by ARO Grant No. DAAD 19-99-1-0317.

¹A. J. Steckl and J. M. Zavada, MRS Bull. **24**, 33 (1999).

²P. N. Favennec, H. L'Haridon, D. Moutonnet, M. Salvi, and Y. LeGuillou, Electron. Lett. **25**, 718 (1989).

³M. Thaik, U. Hommerich, R. N. Schwartz, R. G. Wilson, and J. M. Zavada, Appl. Phys. Lett. **71**, 2641 (1997).

⁴J. M. Zavada, M. Thaik, U. Hommerich, J. D. MacKenzie, C. R. Abernathy, and S. J. Pearton, J. Alloys Compd. **300-301**, 207 (2000).

⁵A. J. Steckl and R. Birkhahn, Appl. Phys. Lett. **73**, 1700 (1998).

⁶D. J. Eaglesham, J. Michael, E. A. Fitzgerald, D. C. Jacobson, J. M. Poate, J. L. Benton, A. Polman, Y.-H. Xie, and L. C. Kimerling, Appl. Phys. Lett. **58**, 2797 (1991).

⁷A. Taguchi, M. Kawashima, K. Takahei, and Y. Horikoshi, Appl. Phys. Lett. **63**, 1074 (1993).

⁸E. Alves, R. C. da Silva, M. F. da Silva, and J. C. Soares, Nucl. Instrum. Methods Phys. Res. B **139**, 313 (1998).

⁹D. S. Lee, J. Heikenfeld, R. Birkhahn, M. Garter, B. K. Lee, and A. J. Steckl, Appl. Phys. Lett. **76**, 1525 (2000).

¹⁰J. D. MacKenzie, C. R. Abernathy, S. J. Pearton, U. Hommerich, X. Wu, R. N. Schwartz, R. G. Wilson, and J. M. Zavada, Appl. Phys. Lett. **69**, 2083 (1996).

¹¹T. Kano, *Phosphor Handbook* (CRC, Boca Raton, FL, 1999), p. 185.